Hindawi
International Journal of Polymer Science
Volume 2022, Article ID 3695462, 16 pages
https://doi.org/10.1155/2022/3695462

Research Article

Synthesis and Properties of a New Type of Terpyridine Cholesterol Derivative Gelator with Applications to Medical Treatments

Lina Qiu,[1,2] **Yang Liu**,[1] **Yunhe Miao**,[1] **Weiwei Zhang**,[2,3] **Aijun Gong**,[1,2] **and Zhipeng Liu**[1]

[1]*School of Chemistry and Biological Engineering, University of Science and Technology Beijing, Beijing 100083, China*
[2]*Basic Experimental Center for Natural Science, University of Science and Technology Beijing, Beijing 100083, China*
[3]*Beijing Key Laboratory for Science and Application of Functional Molecular and Crystalline Materials, University of Science and Technology Beijing, Beijing 100083, China*

Correspondence should be addressed to Aijun Gong; gongaijun5661@ustb.edu.cn

Received 15 February 2022; Revised 11 May 2022; Accepted 30 May 2022; Published 16 June 2022

Academic Editor: M. R. M. Asyraf

Low molecular mass gelators (LMMGs), as a new type of intelligent soft material, possess good response properties to light, electricity, heat, and ultrasound and have many potential applications in fields such as intelligent sensing, biological materials, and drug release. Additionally, steroid derivatives have been a focus in the study of LMMGs for their desirable properties as well, such as their rigid framework, multichiral center, and strong van der Waals accumulation. Furthermore, the coordination ability of terpyridine has been an emphasis in the study of supramolecular chemistry and coordination chemistry as well. Attempts have been made with terpyridine groups that have special responses, such as terpyridine with steroid derivatives, to build more specialized and functional gelators. In this study, we used 2-acetylpyridine, 2-formaldehyde, and cholesterol to synthesize 6-(2,2:6′,2″-terpyridine-4′-carboxamide group) hexanoic acid (with a yield of 64.39%, P1), glycine cholesterol ester (with a yield of 70.36%, P2), and DMTCP (with a yield of 88.92%). Infrared spectroscopy, nuclear magnetic resonance spectroscopy, mass spectrometry, elemental analysis, and gelator performance tests were then conducted to measure the gelation effect of the materials and to explore their gelation mechanisms. Compared to P1 and P2, the DMTCP synthesized by P1 and P2 was able to form gel in more kinds of solvents. In addition, when it contains both terpyridine and cholesterol functional groups, the gelation properties of DMTCP were also significantly improved, and all the gels prepared in the four solvents in which DMTCP can form gels were stimulus responsive.

1. Introduction

Supramolecular chemistry is the chemistry of intermolecular forces and molecular assembly. Ever since Lehn put forward the concept of supramolecular chemistry in 1978 [1], supramolecular chemistry has become a new discipline that has come to intersect with biology, physics, materials, and other disciplines after more than 30 years of rapid development [2, 3]. In recent years, molecular gelators, as an important branch of colloid science, have attracted increasing attention due to their unique supramolecular multistage self-assembly structure and broad application prospects [4, 5]. Low molecular mass gelators (LMMGs) are organic compounds with molecular weights below 2000 that are capable of forming physical gels with solvent molecules with the help of supramolecular self-assembly at low concentrations (mostly less than 3% *w*/*w*) [6–8]. LMMGs based on the supramolecular chemistry principle are a hot topic in current chemistry research [9, 10]. At present, there have been many studies on LMMGs, but there are still great challenges in preparing LMMGs to carry out specific functions.

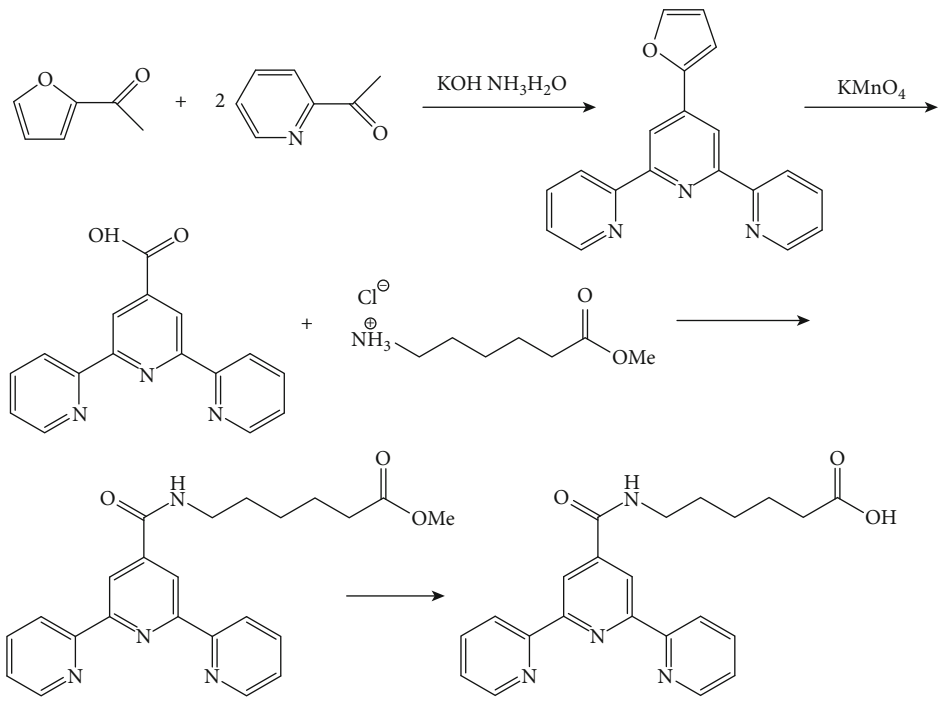

Figure 1: Synthesis route of 6-(2,2′:6′:2″-terpyridine-4′-formamide) hexanoic acid.

Table 1: Elemental composition of 4′-(2-furyl)-2,2′:6′,2″-terpyridine.

	C	H	N	O
Theoretical value	76.24	4.38	14.04	5.34
Actual value	75.97	4.20	13.58	5.20

^{1}H NMR (400 MHz, chloroform-*d*) δ 6.52–6.59 (dd, J = 3.5, 1.8 Hz, 1H), 7.09–7.17 (s, 1H), 7.31–7.43 (t, J = 5.8 Hz, 2H), 7.53–7.62 (s, 1H), 7.82–7.94 (t, J = 7.7 Hz, 2H), 8.59–8.69 (d, J = 8.0 Hz, 2H), and 8.68–8.81 (s, 4H).

Table 2: Elemental composition of 2,2′:6′,2″-terpyridine-4′-carboxylic acid.

	C	H	N	O
Theoretical value	69.31	4.00	15.15	11.54
Actual value	69.10	4.11	15.01	11.32

^{1}H NMR (300 MHz, $CDCl_3$): δ 12.74 (s, 1H), δ 9.18 (d, 2H), δ 8.55 (d, 2H), δ 8.40 (s, 2H), δ 7.74 (t, 2H), and δ 7.23 (t, 2H).

Table 3: Elemental composition of 6-(2,2′:6′,2″-terpyridine-4′-formamide) hexanoic acid methyl ester.

	C	H	N	O
Theoretical value	68.30	5.98	13.85	11.87
Actual value	68.10	5.95	13.65	11.32

^{1}H NMR (400 MHz, DMSO-d_6) δ 1.27–1.42 (d, J = 7.8 Hz, 2H), 1.50–1.64 (q, J = 7.5 Hz, 4H), 2.27–2.37 (t, J = 7.4 Hz, 2H), 3.51–3.63 (s, 3H), 7.48–7.58 (dd, J = 7.3, 5.1 Hz, 2H), 7.98–8.09 (t, J = 7.7 Hz, 2H), 8.60–8.68 (d, J = 8.0 Hz, 2H), 8.72–8.79 (m, 2H), 8.79–8.86 (s, 2H), and 8.99–9.10 (s, 1H).

Table 4: Elemental composition of 6-(2,2′:6′,2″-terpyridine-4′-formamide) hexanoic acid.

	C	H	N	O
Theoretical value	67.68	5.68	14.35	12.29
Actual value	67.30	5.20	13.99	12.32

^{1}H NMR (400 MHz, DMSO-d_6) δ 1.25–1.43 (m, 2H), 1.46–1.69 (dq, J = 14.5, 7.1 Hz, 4H), 2.14–2.30 (t, J = 7.3 Hz, 2H), 7.48–7.58 (dd, J = 7.5, 4.9 Hz, 2H), 7.98–8.09 (dt, J = 7.9, 4.0 Hz, 2H), 8.61–8.67 (d, J = 8.0 Hz, 2H), 8.73–8.79 (d, J = 4.7 Hz, 2H), 8.79–8.84 (s, 2H), 9.00–9.11 (s, 1H), and 11.77–12.09 (s, 1H).

Recent studies have found that the introduction of some special functional groups to gelators can be added to gel materials that have stimulation responses to light, electricity, heat, ultrasonography, fluorescence, pH, magnetic, and fluorine ions. Hence, these materials have great potential applications in various fields such as photosensitive devices, biological materials, drug transport, preparation of nanomaterials, and gel rocket propellants [11–19].

Cholesteric derivatives are a common type of LMMG that are usually classified as cholesterol derivatives or cholic acid derivatives [20–23]. However, the most studied LMMGs are small molecular compounds with cholesterol as their basic structural unit. The main reason for this is due to the rigid structure of cholesterol itself and its strong tendency to cluster orderly in solution. These structures and clusters make cholesterol and its derivatives able to form various aggregation structures in solution easily, and they thus can form supramolecular gelators with different structures and properties. In addition, 2,2′:6′,2″-terpyridine, as one of the most widely used ligands in coordination chemistry, has a strong coordination effect and can form complexes with stable structures with most metals [24–27]. Terpyridine and its derivatives not only have exotic structures but

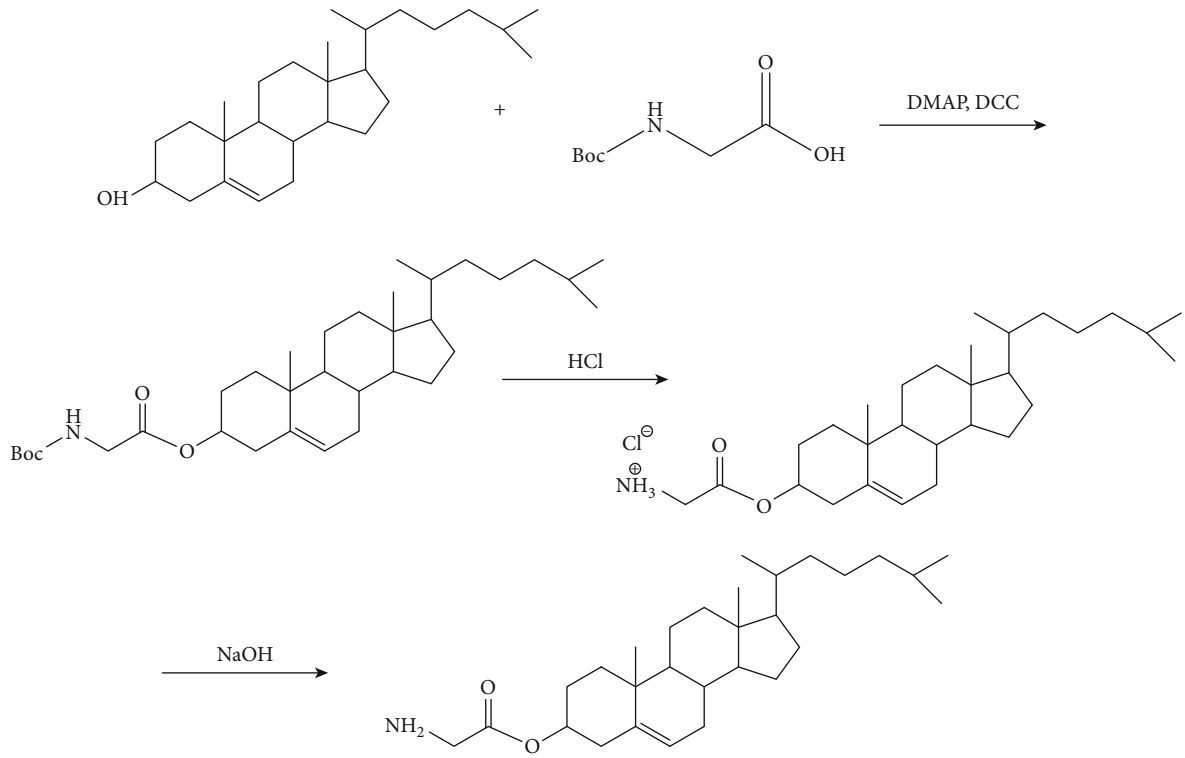

Figure 2: Synthesis route of glycine cholesterol ester.

Table 5: Elemental composition of Boc-glycine cholesterol ester.

	C	H	N	O
Theoretical value	75.09	10.57	2.58	11.77
Actual value	74.56	11.34	2.33	12.56

^{1}H NMR (400 MHz, chloroform-*d*) δ 0.58–0.73 (s, 4H), 0.77–1.67 (m, 56H), 1.90–2.06 (t, J = 15.3 Hz, 3H), 2.24–2.37 (d, J = 8.3 Hz, 3H), 3.81–3.91 (d, J = 5.4 Hz, 2H), 4.60–4.72 (d, J = 9.9 Hz, 1H), and 5.32–5.40 (d, J = 4.9 Hz , 1H).

Table 6: Elemental composition of glycine cholesterol ester hydrochloride.

	C	H	Cl	N	O
Theoretical value	72.54	10.50	7.38	2.92	6.66
Actual value	72.44	12.45	6.58	2.85	8.21

^{1}H NMR (400 MHz, DMSO-d_6) δ 0.62–0.67 (s, 2H), 0.80–0.92 (m, 8H), 0.95–1.00 (s, 3H), 0.98–1.08 (d, J = 18.5 Hz, 1H), 1.05–1.15 (t, J = 10.1 Hz, 4H), 1.27–1.34 (d, J = 8.4 Hz, 2H), 1.32–1.50 (m, 2H), 1.46–1.57 (dd, J = 15.6, 8.5 Hz, 2H), 1.74–1.86 (d, J = 13.0 Hz, 2H), 1.84–2.00 (m, 2H), 2.28–2.34 (d, J = 7.2 Hz, 2H), 3.73–3.80 (d, J = 5.7 Hz, 2H), 4.53–4.62 (m, 1H), 5.19–5.52 (s, 1H), and 8.32–8.37 (s, 2H).

excellent optical, electrical, magnetic, molecular carrying, and catalysis properties as well. The study of terpyridine ligands and complexes (especially the substitutions of those with 4′ positions) has become an important focus of modern coordination chemistry [28–30].

Cholesteric derivatives such as cholesterol have been found to be very effective gelators, and the introduction of terpyridine for metal ion coordination aids in the construction of stimulus-responsive gels. Additionally, a long alkyl chain connection between terpyridine and cholesterol can enhance gelatination. In this paper, we synthesized 6-(2,2′:6′,2″-terpyridine-4′-formamide) hexanoic acid, glycine cholesterol ester, and DMTCP from 2-acetylpyridine, 2-furaldehyde, cholesterol, and Boc-glycine, respectively, and characterized and tested each of their gelator properties. Molecular structures were observed by measuring the infrared spectrum of the synthesized gelators and the xerogel samples prepared in response. The generation, disappearance, or transfer of characteristic peaks in the infrared spectrum indicated the generation of specific groups. Gelation effects were measured by observing the gelation behavior of the synthesized gelators in different organic reagents, and the morphology of the gelators was studied by scanning electron microscope (SEM) in order to explore the gelation mechanism.

Table 7: Elemental composition of glycine cholesterol ester.

	C	H	N	O
Theoretical value	78.50	11.13	3.16	7.21
Actual value	78.32	12.35	3.01	8.32

^{1}H NMR (400 MHz, chloroform-*d*) δ 0.58–0.72 (s, 3H), 0.75–1.66 (m, 34H), 1.66–1.90 (s, 5H), 1.90–2.06 (m, 2H), 2.13–2.50 (d, J = 8.2 Hz, 2H), 3.25–3.53 (s, 2H), 4.53–4.72 (q, J = 11.2, 10.2 Hz, 1H), and 5.27–5.46 (m, 1H).

2. Materials and Methods

2.1. Reagents. We purchased 2-furfural (AR, 99.0%), anhydrous potassium carbonate (AR, 99.0%), anhydrous

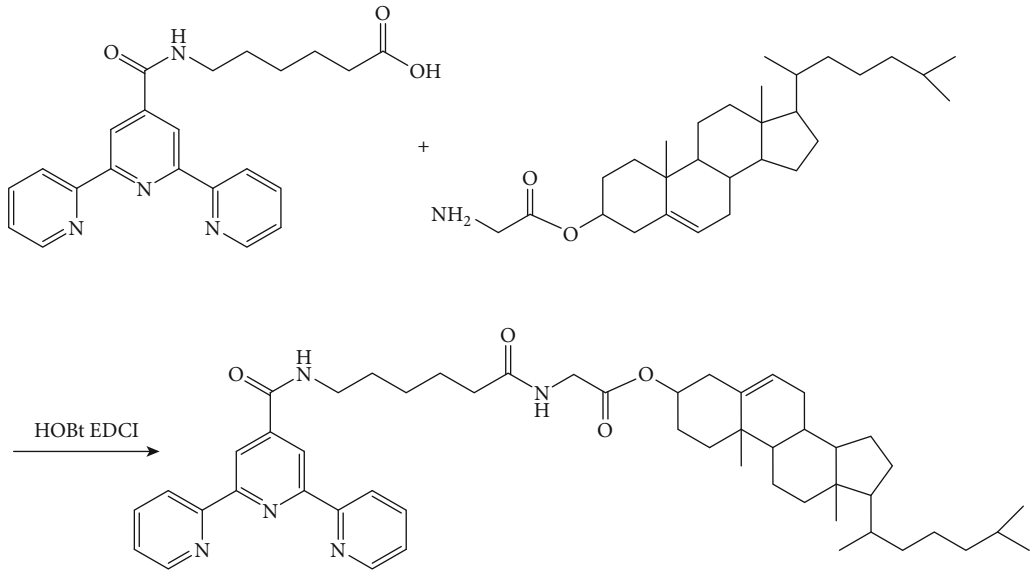

Figure 3: Synthesis route of DMTCP.

Table 8: Elemental composition of DMTCP.

	C	H	N	O
Theoretical value	75.06	8.52	8.58	7.84
Actual value	74.88	7.98	8.45	7.90

^{1}H NMR (400 MHz, chloroform-*d*) δ 0.54–2.04 (m, 43H), 2.15–2.36 (m, 4H), 3.40–3.58 (m, 4H), 3.92–4.03 (d, J = 5.3 Hz, 2H), 4.49–4.61 (m, 1H), 5.23–5.34 (d, J = 19.6 Hz, 1H), 6.18–6.32 (m, 1H), 6.93–7.01 (s, 1H), 7.30–7.39 (m, 2H), 7.80–7.90 (td, J = 7.8, 1.8 Hz, 2H), 8.54–8.62 (d, J = 8.0 Hz, 2H), 8.65–8.72 (q, J = 1.6 Hz, 2H), and 8.72–8.80 (s, 2H).

magnesium sulfate (AR, 99.0%), pyridine (AR, 99.5%), hydrochloric acid (AR, 36.0-38.0%), acetone (AR, 99.5%), sodium thiosulfate pentahydrate (AR, 99.0%), sodium chloride (AR, 99.5%), anhydrous magnesium sulfate (AR, 99.0%), potassium hydroxide (AR, 85%), and potassium permanganate (AR, 99.5%) from Sinopharm Chemical Reagent Co., Ltd. and purchased Boc-glycine (AR, 98.5%), dicyclohexylcarbodiimide (DCC, AR, 99.0%), 4-dimethylaminopyridine (DMAP, AR, 99.0%), 1-benzotriazolol (HOBT, AR, 99.0%), and 1-ethyl-3-(3-dimethylam-inopropyl) carbodiimide hydrochloride (EDCI, AR, 99.0%) from Xiya Reagent Co., Ltd. Absolute ethyl alcohol (AR, 99.7%), dichloromethane (AR, 99.5%), trichloromethane (AR, 99.0%), ethyl acetate (AR, 99.5%), DMF (N,N-dimethylformamide) (AR, 99.7%), tetrahydrofuran (AR, 99.0%) (THF), concentrated sulfuric acid (GR, 95-98%), and petroleum ether (AR) were purchased from Beijing Chemical Works Co., Ltd., and 2-acetylpyridine was purchased from Shanghai Adamas Co., Ltd. Finally, we purchased methyl 6-aminohexanoate hydrochloride from Heowns and cholesterol (AR, 99%) from J&K Scientific Co., Ltd.

2.2. Synthesis of 6-(2,2′:6′,2″-Terpyridine-4′-formamide) Hexanoic Acid (P1). The synthesis route of 6-(2,2′:6′,2″-terpyridine-4′-formamide) hexanoic acid is shown in Figure 1.

2.2.1. Synthesis of 4′-(2-Furyl)-2,2′:6′,2″-terpyridine. We added 9.00 mL (80 mmol) of 2-acetylpyridine, 3.34 mL (40 mmol) of 2-furaldehyde, and 200 mL of anhydrous ethanol to a three-mouth flask. After the solution was stirred evenly, 6.16 g potassium hydroxide and 120 mL ammonia (25%) were then added. Next, the reaction was refluxed overnight at 60°C, and the cooled solution was filtered to obtain the light yellow solid that is the crude product. The crude product was further purified by using silica gel column chromatography with chloroform (or dichloromethane) as the eluent. Finally, the pale yellow eluent was distilled and dried to obtain an orange-yellow, powdery product. The yield of the reaction was 49.27%, and the elemental composition of 4′-(2-furyl)-2,2′:6′,2″-terpyridine is shown in Table 1. We also characterized its molecular structure by ^{1}H NMR. (The same method was applied to subsequent syntheses.)

2.2.2. Synthesis of 2,2′:6′,2″-Terpyridine-4′-carboxylic Acid. We added 3.20 g 4′-(2-furyl)-2,2′:6′,2″-tripyridine and 120 mL pyridine to a conical flask and kept stirring until the solids were completely dissolved. Then, potassium permanganate solution (0.1 g·mL^{-1}) was added drop by drop into the conical flask and stirred at room temperature for 20 h. After the reaction was completed, excessive sodium thiosulfate powder was added to the filtrate of the postreaction solution, and we kept fully stirring until the color turned pale yellow. The solution was left to rest for stratification, and the upper organic phase was reserved to remove solvents by rotary evaporation. After this, 1 mol·L^{-1} sodium hydroxide solution was added, and the remaining solids were dissolved by heating. Then, the solution was filtered to remove the insoluble solids, and concentrated hydrochloric acid was added to the filtrate slowly while fully stirring until a large number of white precipitates appeared. Finally, the white solid product was obtained by washing with deionized water and drying; yield was about 60%. The elemental

Table 9: Solvent gelation behavior of P1 in different organic solvents.

Solvent (polarity)	P1		
	Indoor temperature	70°C	Final state of solution
Water (10.2)	I	I	I
Benzene (2.7)	I	I	I
Methylbenzene (2.4)	I	I	I
Xylene (2.5)	I	I	I
N-Hexane (0.0)	I	I	I
Normal octane	I	I	I
Dodecane	I	I	I
Bromododecane	I	I	I
Dichloromethane (3.4)	I	I	I
Trichloromethane (4.4)	I	I	I
Methyl alcohol (5.1)	I	I	I
Ethyl alcohol (4.3)	I	I	I
1-Octanol	I	I	I
Isopropanol (4.3)	I	I	I
N-Propyl alcohol	I	I	I
Diethyl ether (2.9)	I	I	I
Petroleum ether (0.01)	I	I	I
Ethyl acetate (4.3)	I	I	I
Acetone (5.4)	I	I	I
Acetonitrile (6.2)	I	I	I
Tetrachloromethane (1.6)	I	I	I
Triethylamine (5.0)	I	I	I
1,4-Dioxane (4.8)	I	I	I
Tetrahydrofuran (4.2)	I	S	I
Pyridine (5.3)	S	S	S
DMF (6.4)	S	S	S
DMSO (7.2)	S	S	S

composition of 2,2′:6′,2″-terpyridine-4′-carboxylic acid is shown in Table 2.

2.2.3. Synthesis of 6-(2,2′:6′,2″-Terpyridine-4′-formamide) Hexanoic Acid Methyl Ester. First, we fully dissolved 5.12 g 2,2′:6′,2″-terpyridine-4′-carboxylic acid (18.46 mmol) in 300 mL anhydrous N,N-dimethylformamide (DMF), then added 3.36 g methyl 6-aminohexanoate hydrochloride (18.46 mmol). After that, 7.08 g EDCI (36.92 mmol) was added quickly while stirring at 0°C. Next, the temperature was ambiently raised to room temperature, and the solution was stirred for 12 h and heated to 50°C for 8 h to obtain the light yellow clarification solution. After filtration, the filtrate was dried until the remaining product was viscous, and the solution was then transferred to ethyl acetate/saturated sodium bicarbonate solution = 1/1 (300 mL). After sufficient vibration, the solution was placed in static stratification, and the organic phase was reserved. The aqueous phase was extracted twice with 50 mL ethyl acetate solution, and the organic phase was then recombined with it. After washing the organic phase, we dried it with anhydrous $MgSO_4$ and concentrated it in a vacuum. Then, a white precipitate was formed by adding petroleum ether to the concentrated solution, and the white solid was the product after filtration (yield, 59.32%). The elemental composition of 6-(2,2′:6′,2″-terpyridine-4′-formamide) hexanoic acid methyl ester is shown in Table 3.

2.2.4. Synthesis of 6-(2,2′:6′,2″-Terpyridine-4′-formamide) Hexanoic Acid (P1). Here, we suspended 0.80 g 6-(2,2′:6′,2″-terpyridine-4′-formamide) methyl hexanoate (1.978 mmol) in 150 mL and 1 mol·L^{-1} sodium hydroxide solution and stirred it at room temperature for 14 h to obtain a transparent solution from the reaction. After filtration, the filtrate was reserved, and concentrated hydrochloric acid was added to form a large number of white precipitates. The white solid was then filtered, washed, and dried to obtain the product (yield, 64.39%). The elemental composition of 6-(2,2′:6′,2″-terpyridine-4′-formamide) hexanoic acid is shown in Table 4.

2.3. Synthesis of Glycine Cholesterol Ester. The synthesis route of glycine cholesterol ester is shown in Figure 2.

2.3.1. Synthesis of Boc-Glycine Cholesterol Ester. We dissolved 7.74 g cholesterol (20 mmol) and 3.50 g Boc-glycine (20 mmol) in 350 mL dichloromethane and added 4.12 g

Table 10: Solvent gelation behavior of P2 in different organic solvents.

Solvent (polarity)	P2		
	Indoor temperature	70°C	Final state of solution
Acetonitrile (6.2)	I	I	I
Benzene (2.7)	I	I	I
Methylbenzene (2.4)	I	I	I
Tetrachloromethane (1.6)	I	I	I
N-Hexane (0.0)	I	I	I
N-Octane	I	I	I
Dodecane	I	I	I
Bromododecane	I	I	I
Triethylamine (5.0)	I	I	I
Trichloromethane (4.4)	I	I	I
Methyl alcohol (5.1)	I	I	I
Ethyl alcohol (4.3)	I	I	I
1-Octanol	I	I	I
Isopropanol (4.3)	I	I	I
N-Propyl alcohol (4.0)	I	I	I
Diethyl ether (2.9)	I	I	I
1,4-Dioxane (4.8)	I	I	I
Ethyl acetate (4.3)	I	I	I
Acetone (5.4)	I	I	I
Water (10.2)	I	PS	PS
Xylene (2.5)	S	S	S
Dichloromethane (3.1)	S	S	S
Petroleum ether (0.01)	PS	PS	PS
Tetrahydrofuran (4.0)	G(T)	S	G(T)
Pyridine (5.3)	S	S	S
DMF (6.4)	S	S	S
DMSO (7.2)	I	S	I

dicyclohexylcarbodiimide (DCC) (20 mmol) and 0.24 g 4-dimethylaminopyridine (DMAP) (2 mmol) at 0-2°C. Then, the temperature was ambiently raised to room temperature, and the solution was stirred for 24 h. After the reaction, the postreaction solution was filtered, and the filtrate was washed with hydrochloric acid (0.01 mol·L^{-1}), sodium hydroxide solution (0.01 mol·L^{-1}), and distilled water (50 mL each time) for three times each in turn. After this, we separated the organic phase and dried it with anhydrous $MgSO_4$. Next, a white solid was obtained after the solvent was dried. This crude product was further purified using 200- to 300-mesh silica gel column chromatography with a mixed solvent ($V_{\text{Ethyl acetate}} : V_{\text{Petroleum ether}} = 1 : 6$) as the eluent to afford the first product, which was the target product (yield, 53.34%). The elemental composition of Boc-glycine cholesterol ester is shown in Table 5.

2.3.2. Synthesis of Glycine Cholesterol Ester Hydrochloride. To make the glycine cholesterol ester hydrochloride, we first added 5.44 g Boc-glycine cholesterol ester (10 mmol) to 200 mL dichloromethane. Dry hydrogen chloride gas was slowly injected while stirring until there was no longer any white precipitate being generated. The solution turned into a gel after 30 minutes of rest, and the gel was then stirred to transform it into a solution. After that, a white solid was obtained by filtering, which was the target product (yield, 75.36%). The elemental composition of glycine cholesterol ester hydrochloride is shown in Table 6.

2.3.3. Synthesis of Glycine Cholesterol Ester (P2). For the glycine cholesterol ester (P2), we dissolved 8.52 g glycine cholesterol ester hydrochloride (17.8 mmol) in 300 mL THF and added 2.50 mL triethylamine (17.8 mmol) while stirring. Then, the system was heated to 80°C and refluxed for 5 h. After filtration, the filter residue was removed, and the target product was obtained by distillation under pressure (yield, 70.36%). The elemental composition of glycine cholesterol ester is shown in Table 7.

2.4. Synthesis of DMTCP. The synthesis of DMTCP is shown in Figure 3.

To synthesize the DMTCP, we dissolved 0.3900 g 6-(2,2′:6′,2″-terpyridine-4′-formamide) caproic acid (1 mmol) and 0.1351 g HOBT (1 mmol) in 15 mL DMF and dissolved

Table 11: Gelation behavior of DMTCP in different organic solvents.

Solvent	DMTCP		
	Indoor temperature	70°C	Final state of solution
Benzene	I	I	I
Methylbenzene	I	I	I
N-Hexane	I	I	I
N-Octane	I	I	I
Dodecane	I	I	I
Triethylamine	I	I	I
Trichloromethane	I	I	I
Methyl alcohol	I	I	I
Ethyl alcohol	I	I	I
1-Octanol	I	I	I
Isopropanol	I	I	I
N-Propyl alcohol	I	I	I
Ethyl acetate	I	I	I
Petroleum ether	I	I	I
Water	I	I	I
Tetrachloromethane (1.6)	I	S	G (transparency)
Bromododecane	I	S	G (transparency)
Diethyl ether (2.9)	I	I	G (turbidity)
Xylene (2.5)	I	S	G (transparency)
Acetone (5.4)	I	S	I
Acetonitrile (6.2)	I	S	I
1,4-Dioxane (4.8)	S	S	S
Dichloromethane (4.4)	S	S	S
Tetrahydrofuran (4.2)	S	S	S
Pyridine (5.3)	S	S	S
DMF (6.4)	S	S	S
DMSO (7.2)	S	S	S

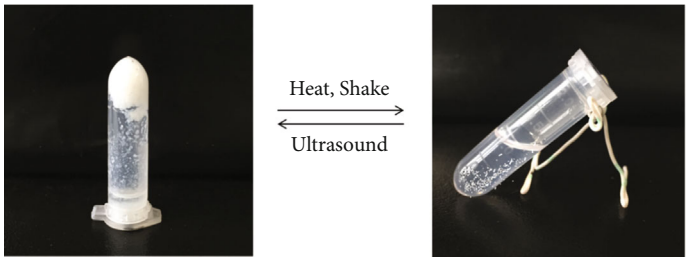

Figure 4: Changes of DMTCP (diethyl ether) gel-sol.

0.5320 g cholesterol glycine ester (1.2 mmol) and 0.3834 g EDCI (2 mmol) in 60 mL DCM at the same time. Next, the two solutions were mixed and stirred at 30°C for 24 h. After the reaction, we obtained the reaction product by rotatory evaporation and then added 30 mL DCM to dissolve it. The product was washed with 100 mL deionized water three times, and the organic phase was retained. After rotatory evaporation, the product was then purified on a silica gel column (methanol : DCM = 2 : 5). Finally, we obtained pure DMTCP (yield, 88.92%). The elemental composition of DMTCP is shown in Table 8.

2.5. Methods. After the above chemical syntheses, FT-IR P1, P2, DMTCP, and the gels formed by them were pressed together with KBr and tested with the FT-IR 8400 SHIMADZU Fourier transform infrared spectrometer. However, because P1 failed to form a gel in the experimental organic solvent, the correlation spectrum of gel formed by P1 could not be created.

2.5.1. Preparation of Xerogel. The gels formed by P2 or DMTCP were placed on an ultraclean platform, and the ventilation hood was opened until all the organic solvents in the

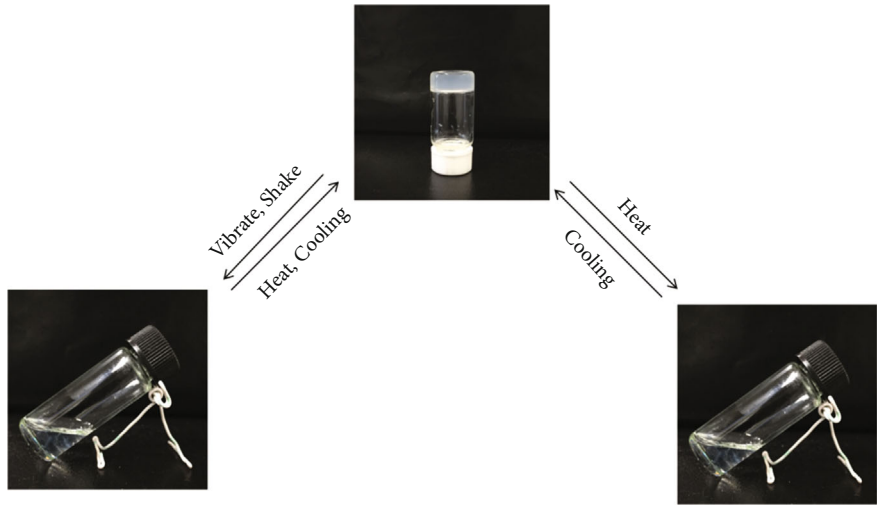

Figure 5: Gel-sol transition diagram of DMTCP (CCl_4, bromodecane, and xylene).

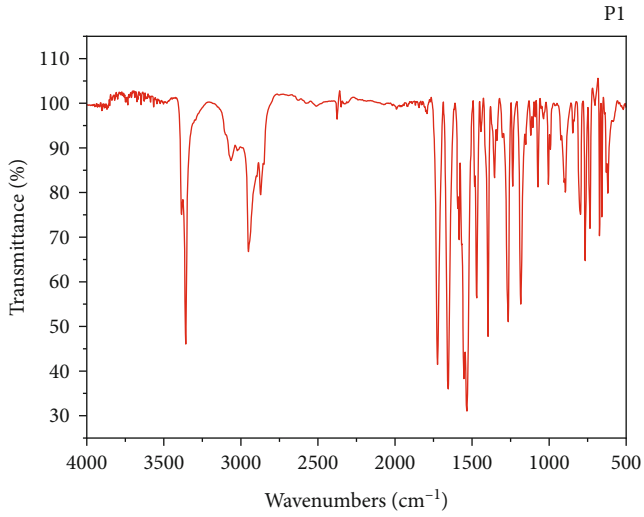

Figure 6: Infrared spectra of 6-(2,2′:6′:2″-terpyridine-4′-formamide) hexanoic acid.

gel were removed so that the resulting xerogel could be used for SEM analysis. Since the boiling point of bromododecane is 276°C, the gel prepared with bromododecane was put into the drying oven overnight at 100°C to the xerogel.

2.5.2. SEM. The sample used for SEM analysis was sprayed with gold for 200 s prior to being observed. The acceleration voltage of the SEM test was set to 5 kV, and the emission current was set to 100 μA.

2.5.3. Gelation Test. The gelation properties of P1, P2, and DMTCP in different solvents were tested by the method of "tube inversion." That is, after the heating and cooling treatment of the solvent were inverted, would the solvent flow to form a gel? A total of 27 common solvents in the laboratory were selected for the gelation tests, and 0.0250 g P1, P2, or DMTCP and 1 mL solvent were added into a 5 mL sample tube (sample concentration was 2.5% (W/V)).

When a gel system formed after being dissolved completely and being placed at room temperature, it was denoted by "GT" and a gel system formed by heating and cooling as "G." A system in which the solute could not be dissolved even at the boiling point was called an insoluble system, "I," and one in which it partially dissolved was denoted as "PS." Finally, a system that completely dissolved was denoted as "S." The experimental results are shown in Tables 9, 10, and 11.

2.5.4. Critical Gel Concentration (CGC) Test. The critical gel concentration was measured by the control variate method. Here, 1 mL solvent was added into a 5 mL sample tube, and the amount of gelator was then increased successively from 1 mg in 1 mg increments until a gel was formed. After heating, cooling, and standing, the minimum amount of gelator required to form a gel was recorded.

2.5.5. Thermal Stability Analysis of Gels. To analyze the thermal stability of the gels, we first performed a gel-sol phase transition temperature (T_{gel}) test. The gel was placed in a sealed 5 mL sample bottle and immersed upside down in a water bath that was heated at 1°C·min^{-1} from 25°C. Then, the bottle was tilted and the temperature (T_{gel}) was noted as the state of the gel began to change. Each gelation concentration was tested three times in parallel to reduce error. Additionally, T_{gel} was tested in different concentrations of gelators and solvents to analyze the thermal stability more comprehensively.

3. Results and Discussion

3.1. Gelation Behaviors of the Compounds. As we can see from Table 9, P1 was insoluble in all tested solvents except pyridine, DMF, and DMSO (but was soluble under heating conditions in THF), showing a poor solubility among the gel solvents we tried. Because P1 could not be dissolved in so many solvents, the spatial network structure could not be formed. Hence, P1 could not be prepared as a gel with

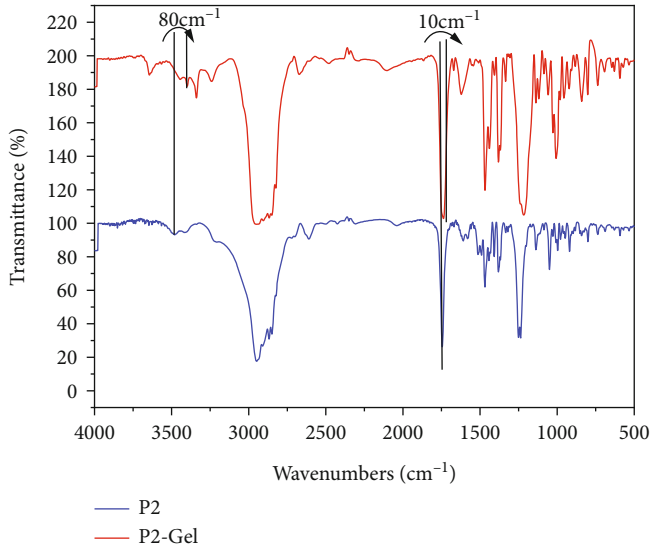

Figure 7: Infrared contrast spectra of P2 and P2-Gel.

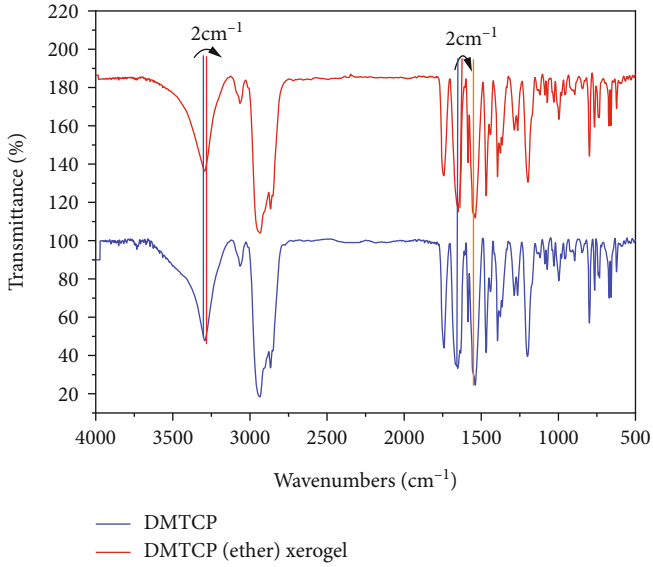

Figure 8: Infrared comparison between DMTCP (ether) xerogel and DMTCP.

these solvents. However, in the solvents that could dissolve P1, it was completely dissociated in the solvent and the interaction between the solute and P1 was weak. As a result, the network structures necessary for preparing gels could not be formed.

The solvent gelation experiments for P2 in 27 solvents showed that P2 only formed a gel in THF (Table 10). Furthermore, there were two ways it could generate a gel. The first was that a gel could be formed after ultrasonic treatment at room temperature. The other was that a gel could be formed after heating and cooling without ultrasonic treatment. In addition, the gel formed with the latter method could return to its solution state after heating and violent shaking, but this gel could be formed again after heating and cooling.

By comparing the polarity between solvents, we found that P2 exhibited a medium polarity. The P2 could dissolve in the solvents with a similar polarity to THF (4.2), such as xylene (2.5), dichloromethane (3.4), pyridine (5.3), DMF (6.4), and DMSO (7.2). This can be explained on the microscopic level: when the interaction between disperse phases that is weaker than that between disperse phase and dispersant, the P2 appears as a solution. Conversely, the dispersions can also aggregate to form precipitates.

The results of the gelation test (Table 11) indicate that DMTCP was insoluble in ethyl ether at room temperature and under heating conditions. However, in the concentration of 10‰ (w/v), the DMTCP was able to form an opaque gel after 20 seconds of ultrasonic processing (Figure 4). In other words, DMTCP (diethyl ether) gel had a special

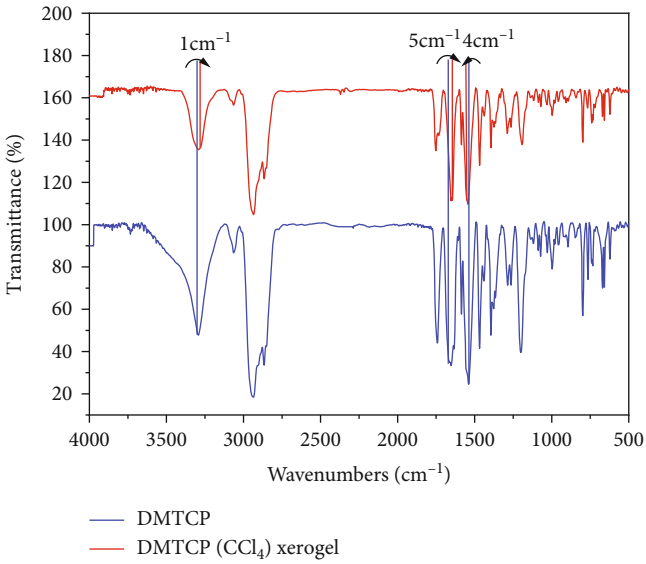

Figure 9: Infrared comparison between DMTCP(CCl_4) xerogel and DMTCP.

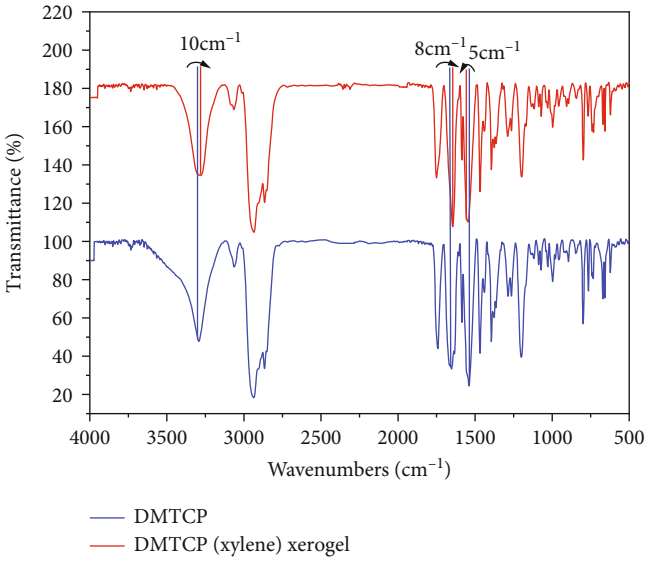

Figure 10: Infrared comparison between DMTCP (xylene) xerogel and DMTCP.

response to ultrasound. Unfortunately, the gel did not possess the property of thermal reversibility.

In contrast, DMTCP could dissolve in carbon tetrachloride, dodecane bromide, and xylene to form a clear solution under heating conditions. After ambient cooling, it could also form a transparent gel.

Furthermore, the gels we tested that formed in carbon tetrachloride, dodecane bromide, and xylene had the same properties. They could be transformed from a solution into a gel by heating and cooling; they were thermally reversible. In addition, under the action of shear stress, they could be transformed from the gel state to the solution state, but could not be automatically transformed into a gel at room

Figure 11: Macroscopic view of P2 forming a gel in THF.

temperature. However, they were able to convert to gels after being heated and cooled, and this could be repeated several times (Figure 5).

3.2. Spectroscopy. The infrared spectrum of compound 6-(2,2′:6′,2″-terpyridine-4′-formamide) hexanoic acid is shown in Figure 6, where we can see that the absorption peak at 3357 cm^{-1} is N-H stretching vibration absorption of the secondary amide. At 3064 cm^{-1}, there is a wide peak center, which is the characteristic absorption peak of carboxylic acid, and at 1720 cm^{-1}, the wide peak absorption indicates the existence of carboxylic acid. The absorption peaks at 2950 cm^{-1} and 2871 cm^{-1} are the stretching vibration absorption of saturated alkanes, and the peak at 1654 cm^{-1} is the stretching vibration absorption of the carbonyl group C=O, which also reflects the association absorption peak of the compound's amide bond. The four peaks at 1583 cm^{-1}, 1552 cm^{-1}, 1533 cm^{-1}, and 1469 cm^{-1} are the characteristic absorption of pyridine ring skeleton vibration. Hence, when we combined this analysis with our ^{1}H NMR analysis, we determined the product to indeed be target product P1.

From the structural analysis we conducted, we found that one end of P1 was terpyridine, which itself forms a large conjugated system but has poor solubility. The long chain of hexanoic acid at the other end and the long chain of carbon can reduce the polarity of the material, but the overall polarity of the material was higher. Thin layer chromatography also showed that only by increasing the amount of methanol in the developing agent can it be developed.

As we can see from the comparison between P2 and P2-Gel in Figure 7, after P2 formed the gel, two absorption peaks formed by the stretching vibration of the primary amine at 3485 cm^{-1} and 3413 cm^{-1} appear at 3398 cm^{-1} and 3338 cm^{-1}, respectively. In addition, the peak became wider. Additionally, the stretching vibration absorption peaks of the carbonyl group in the ester group at 1745 cm^{-1} appear at 1735 cm^{-1}. Under the influence of hydrogen bonds, these peaks move to the direction of the small wave numbers, which directly indicates the existence of hydrogen bonds in the formed gel. We conclude that the position of the hydrogen bonds in P2 should be between the primary amine group and the ester carbonyl group.

Figure 8 shows that the N-H stretching vibration absorption peak in the amide bond located at 3292 cm^{-1} moved 2

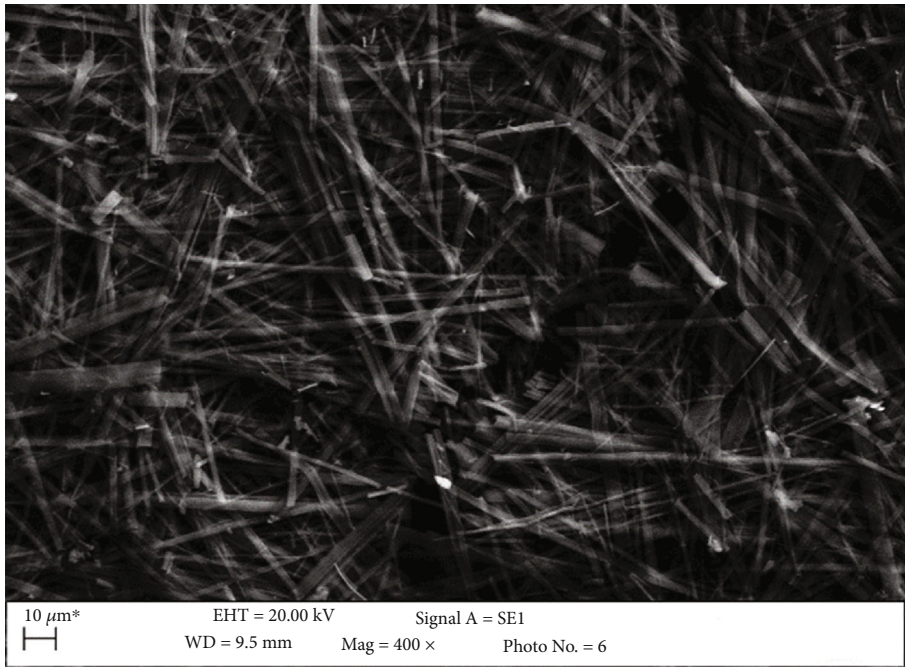

(a)

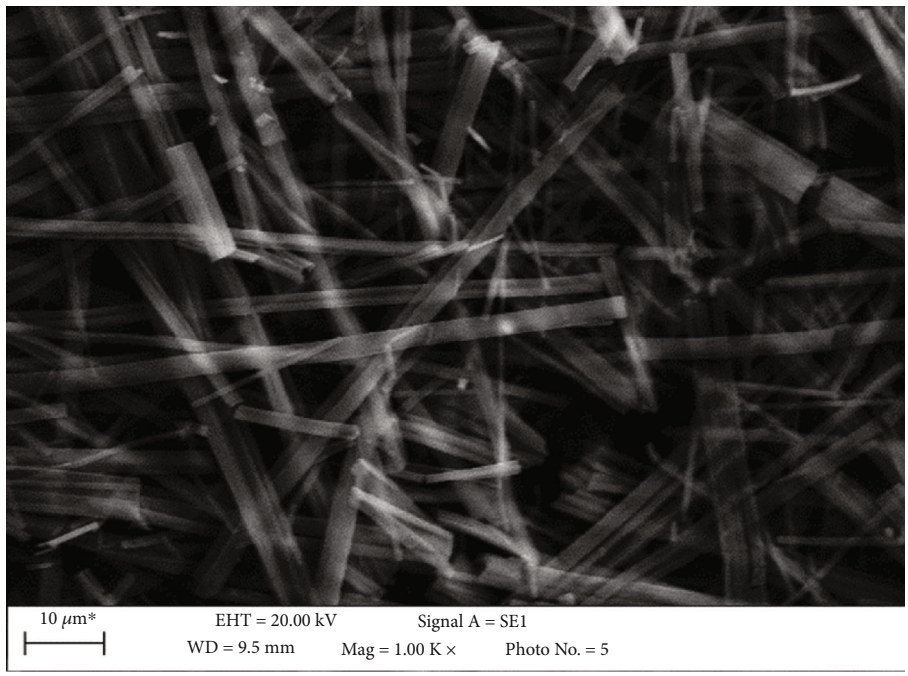

(b)

Figure 12: SEM image of P2 xerogel (THF) at 400 times (a) and 1000 times (b) magnification.

units to the direction of the low wave numbers after the formation of the gel and that the C=O stretching vibration absorption peak of the amide bond at 1652 cm^{-1} moved to 1650 cm^{-1} in the xerogel. The bending vibration peak of N-H in the amide bond at 1539 cm^{-1} stayed the same. Moreover, the C=O stretching vibration peak of the ester group at 1741 cm^{-1} moved to 1743 cm^{-1}, which is an abnormal move to the direction of higher wave numbers. According to the above data, DMTCP may form a weak hydrogen bond in diethyl ether.

In Figure 9, we see that after gel formation in CCl_4, the N-H stretching vibration absorption peak of the amide bond at 3292 cm^{-1} moved toward the low wave numbers, at 3291 cm^{-1}, with a slight red shift, and that the C=O stretching vibration absorption peak at 1652 cm^{-1} in the amide bond moved to 1647 cm^{-1} in the xerogel. That is, it moved 5 units towards the lower wave numbers. The N-H bending vibration peak in the amide bond at 1539 cm^{-1} moved to the higher wave numbers and reached 1543 cm^{-1}. This shows that hydrogen bonds were formed between the amide bonds.

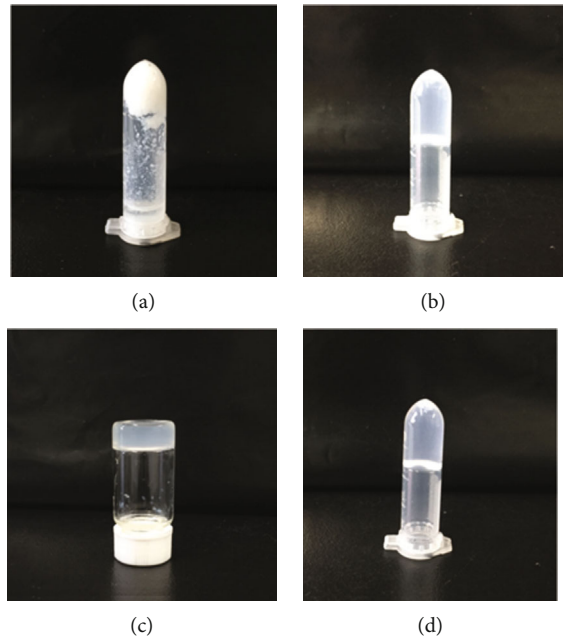

Figure 13: Macroscopic morphology of DMTCP gel formed in four solvents: (a) diethyl ether, (b) carbon tetrachloride, (c) bromododecane, and (d) xylene.

Figure 10 shows that the N-H stretching vibration absorption peak of the amide bond at 3292 cm^{-1} moved to the lower wave numbers to the point at 3282 cm^{-1} after the gel was formed in xylene (red shift). The C=O stretching vibration absorption peak at 1652 cm^{-1} in the amide bond moved to 1644 cm^{-1} in the xerogel. In other words, it moved 8 units towards the lower wave numbers. Additionally, the N-H bending vibration peak in the amide bond at 1539 cm^{-1} moved toward the higher wave numbers and reached 1544 cm^{-1}. This shows that hydrogen bonds were formed between the amide bonds, as in Figure 9.

3.3. Morphology. The macroscopic characteristics of the gel formed by P2 are shown in Figure 11. As can be seen from the figure, it was an opaque gel in the THF solvent, with an obvious solvent gelation effect. There also were no free solvent flows after inversion.

The microcosmic characteristics of the gel are shown in Figure 12. From the scanning electron microscopy (SEM) images of the P2-Gel at 400 times (Figure 12(a)) and 1000 times (Figure 12(b)) magnification, we can see that P2 formed a fibrous gelatinous structure in the THF solvent. Based on the hydrogen bond formation mechanism of the P2-Gel mentioned above, we can further infer that the hydrogen bond between primary amines formed the ester carbonyl group. The promoted fibers between P2 molecules formed a three-dimensional network structure and bound with the THF solvent to form a gel.

The macroscopic characteristic diagram of the gel formed by DMTCP in different organic solvents is shown in Figure 13.

As we can see from Figures 14(a) and 14(b), DMTCP formed a densely interlaced and extremely fine fibrous structure in diethyl ether that was also very disorderly. This is consistent with the appearance of the opaque gel that DMTCP formed under ultrasonic in diethyl ether as well, and we speculate that DMTCP molecules stack themselves through hydrogen bonding under intense ultrasonic vibration. In addition, the intermolecular interactions between ether and DMTCP are balanced. That is, the intermolecular interactions between solute and solvent are balanced, and these balanced intermolecular interactions prevent DMTCP from forming its own excessive agglomeration to form precipitation and from sufficient dispersion in ether to establish a spatial network. Therefore, DMTCP has ultrasonic response characteristics in ethyl ether and forms an opaque gel, which is the macroscopic representation of the balanced intermolecular interactions between the dispersed substance and the dispersant.

Figures 14(c) and 14(d) show the SEM images of DMTCP (carbon tetrachloride) xerogel at 500 and 7K magnification, respectively. At lower magnification, we can see that the surface of the gel is tight but wrinkled. At 7K magnification, however, we can see that DMTCP forms flat banded fiber bundles in carbon tetrachloride, and the amide bond structure in the molecular structure is one of the factors that promote the process of solvent gelation.

Figures 14(e) and 14(f) show the SEM images of gels formed by DMTCP in bromododecane and xylene, but the clear microstructure of xerogel cannot be seen. Reasons for this may include the following. First, it may be that because of the high boiling point of bromododecane and xylene, it is difficult to volatilize the solvent at room temperature. Hence, the method of solvent evaporation by high temperature heating was used. The high temperature makes the solvent outside the gel evaporate rapidly, however, which may lead to the rapid collapse and contraction of the gel structure. The xerogel therefore may have appeared to form a denser structure so that the microstructure could not be observed.

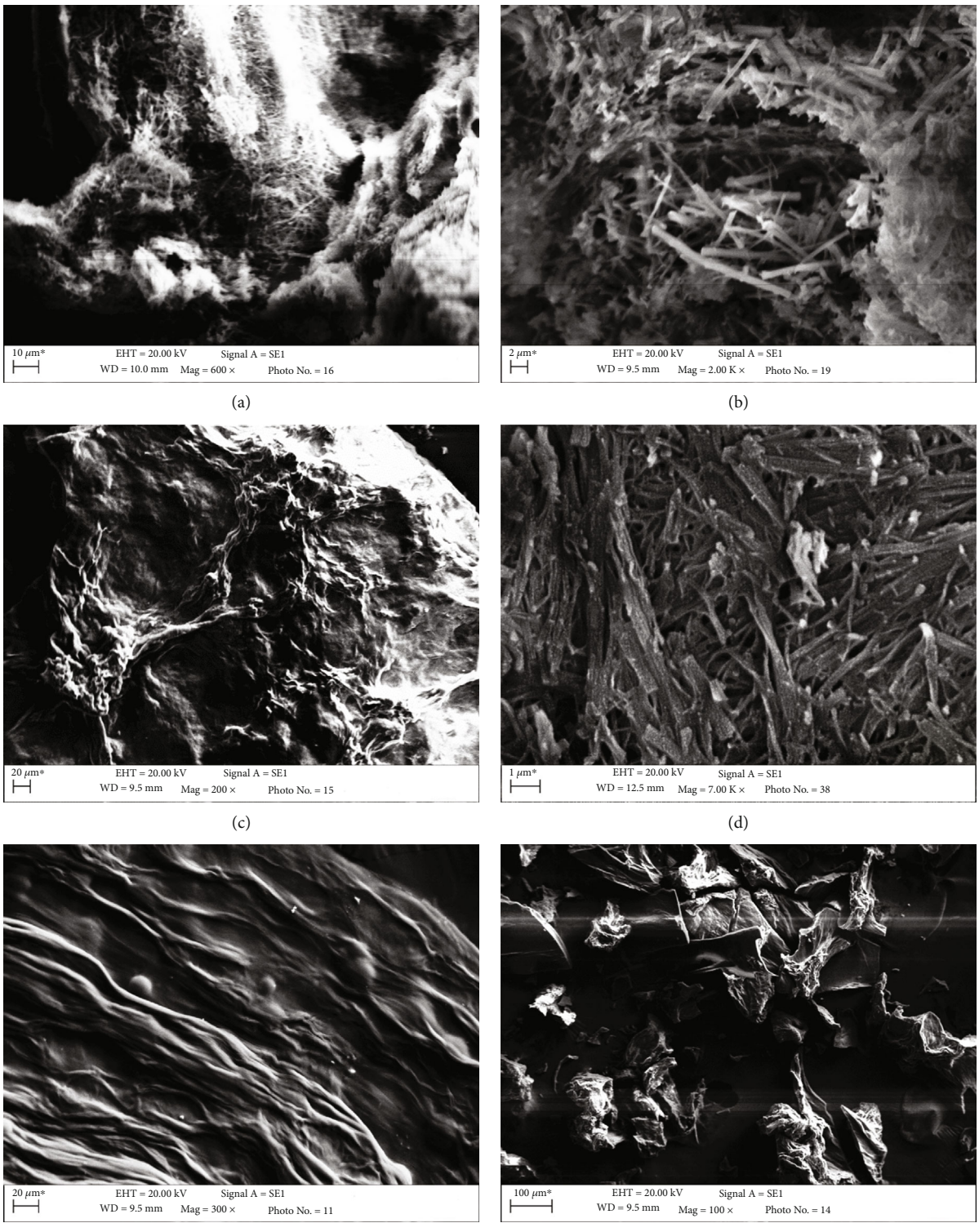

Figure 14: (a) 600-fold SEM diagram of DMTCP (ethyl ether), (b) 1.5K SEM diagram of DMTCP (ethyl ether), (c) DMTCP (CCl_4) 500 times SEM, (d) DMTCP (CCl_4) 7K times SEM, (e) DMTCP($CH_3(CH_2)_{11}Br$) 300 times SEM, and (f) DMTCP (DMB) 100 times SEM.

Second, macroscopically, the transparent gels formed by them is relatively tight, and this may be because the structures themselves are closely connected. As a result, the microstructure could not be observed after drying and agglomeration.

3.4. Properties of Gelation

3.4.1. Critical Gel Concentration (CGC) Test. The CGC test results show that the CGC of P2 in THF was 6‰ (w/v). Since DMTCP had good gelation behavior in diethyl ether,

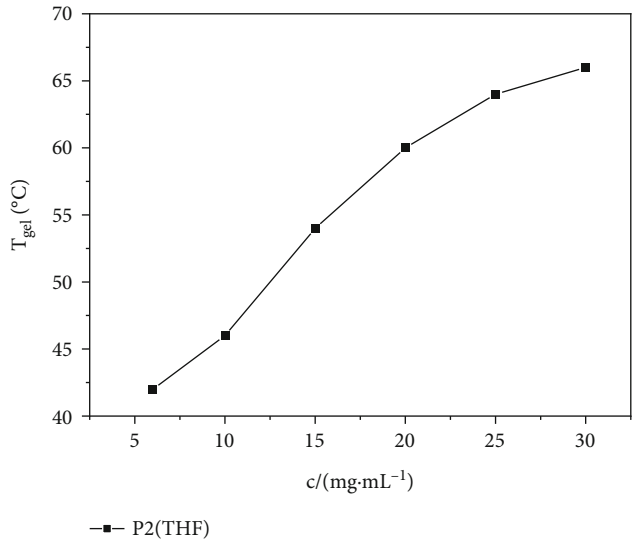

Figure 15: P2 (THF) gel-sol phase transition temperature diagram.

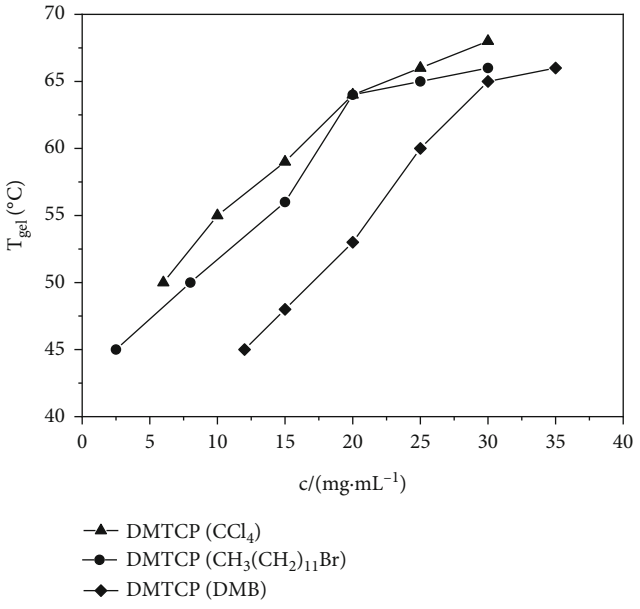

Figure 16: Gel-sol phase transition temperature diagram of DMTCP.

carbon tetrachloride, bromododecane, and xylene, the CGCs of these four kinds of gels were each tested. The final experiment showed that the CGCs of DMTCP in the four solvents were $CGC_{ether} = 10‰(W/V)$, $CGC_{carbon\ tetrachloride} = 6‰(W/V)$, $CGC_{bromododecane} = 2.5‰(W/V)$, and $CGC_{xylene} = 12‰(W/V)$, and from this, we see that DMTCP had the lowest critical gel concentration in bromododecane.

3.4.2. Thermal Stability Analysis of Gels. In our thermal stability analysis, we tested T_{gel} in different concentrations of P2 in THF. Figure 15 shows that T_{gel} increased with the concentration of P2, and this indicates that the higher the gelator concentration, the tighter the gel accumulation and the better the thermal stability.

Due to the thermally reversible properties of the gels formed by DMTCP in the three organic solvents we tested, we tested the gel-sol phase transition temperature (T_{gel}) as well in different concentrations of DMTCP in carbon tetrachloride, bromododecane, and xylene, and the results are shown in Figure 16. Here, we see that T_{gel} increased with the concentration of DMTCP in all three organic solvents, and this also indicates that the higher the gel factor concentration, the closer the gel accumulation and the better the thermal stability.

4. Conclusions

We designed and synthesized three LMMGs, named 6-(2,2′:6′,2″,-terpyridine-4′-formylamino) hexanoic acid (P1), glycine cholesterol ester (P2), and DMTCP, for this paper and conducted infrared spectroscopy, nuclear magnetic resonance spectroscopy, mass spectrometry, elemental analysis, and gelation performance tests on each of them. Our conclusions are as follows. First, glycine cholesterol ester (P2) was able to form opaque gels in the THF solution that could be transformed into a solution under the action of heat and shear stress. The P2 also had thermal reversibility and could form gels repeatedly. Additionally, based on infrared spectrum and SEM image analysis, hydrogen bonds are the main driving force for the formation of gelator clusters. Pang et al. [31] have also mentioned that directional hydrogen bonding is helpful to the formation of aggregates.

Second, DMTCP, synthesized from P1 and P2, could gelate the solvents diethyl ether, carbon tetrachloride, xylene, and bromododecane. Compared to P2 and P1, DMTCP not only introduced the terpyridine functional group into the cholesterol group but also significantly improved gelation. The gelators in the four solvents were stimulus responsive and achieved the desired effects as well. Third, the infrared spectrum analysis of each xerogel formed by DMTCP showed that the hydrogen bonds were still the main driving force of gelator formation, and the SEM image analysis of gelators formed by the four solvents showed that the micromorphology of each of the gelators formed by the same gelata in different solvents was also different.

The gel formed by DMTCP not only provided a very stable structure for binding metal ions but also contained cholesterol groups with good biofilm compatibility. Currently, ruthenium complexes of terpyridine have been used in gene therapy [32], and the gel formed by the complexation of the terpyridine group and other metal ions may well advance the study of drug release. In addition, the biofilm compatibility provided by cholesterol gives DMTCP potential research significance in the directional supply of metal ions.

Data Availability

No data were used to support this study.

Conflicts of Interest

The authors declare that they have no conflicts of interest.

Acknowledgments

This study was financially supported by the National Key R&D Program of China, No. 2017YFF0106006, and the Natural Science Foundation of Beijing Municipality, No. 8172033.

Supplementary Materials

(1) ^{1}H-NMR spectra of 4′-(2-furyl)-2,2′:6′,2″-terpyridine. (2) ^{1}H-NMR spectra of 2,2′:6′,2″-terpyridine-4′-carboxylic acid. (3) ^{1}H-NMR spectra of 6-(2,2′:6′,2″-terpyridine-4′-formamide) caproic acid. (4) ^{1}H-NMR spectra of Boc-glycine cholesterol ester. (5) ^{1}H-NMR spectra of glycine cholesterol ester. (6) ^{1}H-NMR spectra of DMTCP. (7) Mass spectrometry of 4′-(2-furyl)-2,2′:6′,2″-terpyridine. (8) Mass spectrometry of 2,2′:6′,2″-terpyridine-4′-carboxylic acid. (9) Mass spectrometry of 6-(2,2′:6′,2″-terpyridine-4′-formamide) caproate methyl ester. (10) Mass spectrometry of 6-(2,2′:6′,2″-terpyridine 4′-formamide) caproic acid. (11) Mass spectrometry of Boc-glycine cholesterol ester. (12) Mass spectrometry of glycine cholesterol ester. (13) Mass spectrometry of DMTCP. *(Supplementary materials)*

References

[1] J. M. Lehn, "Inclusion complexes of macropolycyclic receptor molecules," *Pure and Applied Chemistry*, vol. 50, pp. 871–892, 1978.

[2] F. Huang and E. V. Anslyn, "Introduction: supramolecular chemistry," *Chemical Reviews*, vol. 115, no. 15, pp. 6999-7000, 2015.

[3] R. T. Eduardo, "Supramolecular gels," *Nano Design for Smart Gels*, pp. 35–69, 2019.

[4] D. Xuewen and J. Zhou, "Supramolecular hydrogelators and hydrogels: from soft matter to molecular biomaterials," *Chemical Reviews.*, vol. 115, no. 24, pp. 13165–13307, 2015.

[5] S. Bhattacharya and S. K. Samanta, "Soft-nanocomposites of nanoparticles and nanocarbons with supramolecular and polymer gels and their applications," *Chemical Reviews*, vol. 116, no. 19, pp. 11967–12028, 2016.

[6] R. G. Weiss, "The past, present, and future of molecular gels. What is the status of the field, and where is it going?," *Journal of the American Chemical Society*, vol. 136, no. 21, pp. 7519–7530, 2014.

[7] M. George, "Molecular organogels. Soft matter comprised of low-molecular-mass organic gelators and organic liquids," *Accounts of Chemical Research*, vol. 39, no. 8, pp. 489–497, 2006.

[8] N. Yan, "Pyrenyl-linker-glucono gelators. Correlations of gel properties with gelator structures and characterization of solvent effects," *Langmuir*, vol. 29, no. 2, pp. 793–805, 2013.

[9] Y. Chunmeng, "Terthiophene derivatives of cholesterol-based molecular gels and their sensing applications," *Langmuir*, vol. 30, no. 5, pp. 1257–1265, 2014.

[10] W. Cheng, "A low-molecular-mass gelator with an electroactive tetrathiafulvalene group: tuning the gel formation by charge-transfer interaction and oxidation," *Journal of the American Chemical Society*, vol. 127, no. 47, pp. 16372-16373, 2005.

[11] N. D. Bansode, K. R. Sindhu, C. Morel et al., "A disulfide based low molecular weight gel for the selective sustained release of biomolecules," *Biomaterials Science*, vol. 8, no. 11, pp. 3186–3192, 2020.

[12] M. Lakdusinghe, M. Abbaszadeh, S. Mishra et al., "Nanoscale self-assembly of poly(3-hexylthiophene) assisted by a low-molecular-weight gelator toward large-scale fabrication of electrically conductive networks," *ACS Applied Nano Materials*, vol. 4, no. 8, pp. 8003–8014, 2021.

[13] J. N. Loos, C. E. Boott, D. W. Hayward, G. Hum, and M. J. MacLachlan, "Exploring the tunable optical and mechanical properties of multicomponent low-molecular-weight gelators," *Langmuir*, vol. 37, no. 1, pp. 105–114, 2021.

[14] F. Gelain, Z. Luo, and S. Zhang, "Self-assembling peptide Eak16 and Rada16 nanofiber scaffold hydrogel," *Chemical Reviews*, vol. 120, no. 24, pp. 13434–13460, 2020.

[15] M. Abbas, W. P. Lipiński, J. Wang, and E. Spruijt, "Peptide-based coacervates as biomimetic protocells," *Chemical Society Reviews*, vol. 50, no. 6, pp. 3690–3705, 2021.

[16] B. O. Okesola, Y. Wu, B. Derkus et al., "Supramolecular self-assembly to control structural and biological properties of multicomponent hydrogels," *Chemistry of Materials*, vol. 31, no. 19, pp. 7883–7897, 2019.

[17] A. Chalard, M. Mauduit, S. Souleille, P. Joseph, L. Malaquin, and J. Fitremann, "3D printing of a biocompatible low molecular weight supramolecular hydrogel by dimethylsulfoxide water solvent exchange," *Additive Manufacturing*, vol. 33, p. 101162, 2020.

[18] E. R. Draper, B. Dietrich, K. McAulay et al., "Using small-angle scattering and contrast matching to understand molecular packing in low molecular weight gels," *Matter*, vol. 2, no. 3, pp. 764–778, 2020.

[19] D. Bordignon, B. Lonetti, C. Coudret et al., "Wet spinning of a library of carbohydrate low molecular weight gels," *Journal of Colloid and Interface Science*, vol. 603, pp. 333–343, 2021.

[20] H. Svobodová, V. Noponen, E. Kolehmainen, and E. Sievänen, "Recent advances in steroidal supramolecular gels," *RSC Advances*, vol. 2, no. 12, pp. 4985–5007, 2012.

[21] M. Zhang, S. Strandman, K. C. Waldron, and X. X. Zhu, "Supramolecular hydrogelation with bile acid derivatives: structures, properties and applications," *Journal of Materials Chemistry B*, vol. 4, no. 47, pp. 7506–7520, 2016.

[22] P. Dastidar, "Supramolecular gelling agents: can they be designed?," *Chemical Society Reviews*, vol. 37, no. 12, pp. 2699–2715, 2008.

[23] S. Papri and M. T. Kumar, "Coordination polymer gels: soft metal–organic supramolecular materials and versatile applications," *Chemical Communications*, vol. 52, no. 52, pp. 8055–8074, 2016.

[24] F. KrÖhnke, "The specific synthesis of pyridines and oligopyridines[1]," *Synthesis*, vol. 1976, no. 1, pp. 1–24, 1976.

[25] J. S. Choi, C. W. Kang, K. Jung, J. W. Yang, Y.-G. Kim, and H. Han, "Synthesis of DNA triangles with vertexes of bis(terpyridine)iron(II) complexes," *Journal of the American Chemical Society*, vol. 126, no. 28, pp. 8606-8607, 2004.

[26] D. Wang, H. Wang, and H. Li, "Novel luminescent soft materials of terpyridine-containing ionic liquids and europium(III)," *ACS Applied Materials & Interfaces*, vol. 5, no. 13, pp. 6268–6275, 2013.

[27] S. Yuan, H.-B. Chen, Y. Zhang, and J. Pei, "Rigid linear and star-shaped π-conjugated 2,2′:6′,2″-terpyridine ligands with blue emission," *Organic Letters*, vol. 8, no. 25, pp. 5701–5704, 2006.

[28] E. Rajalakshmanan and V. Alexander, "Synthesis, luminescence, and electrochemical studies of tris(homoleptic) ruthenium(II) and osmium(II) complexes of 6′-tolyl-2,2′:4′,2″-terpyridine," *Inorganic Chemistry*, vol. 46, no. 16, pp. 6252–6260, 2007.

[29] M. Mura and F. Silly, "Experimental and theoretical analysis of hydrogen bonding in two-dimensional chiral 4′,4′-(1,4-phenylene)bis(2,2′:6′,2″-terpyridine) self-assembled nanoarchitecture," *The Journal of Physical Chemistry C*, vol. 119, no. 48, pp. 27125–27130, 2015.

[30] C. Andrew, "Comparison of the photophysical properties of osmium(II) bis(2,2′:6′,2″-terpyridine) and the corresponding ethynylated derivative," *The Journal of Physical Chemistry A*, vol. 109, no. 10, pp. 2302–2309, 2005.

[31] S. Pang, H. Chen, Z. Jiang et al., *Water-in-oil emulsion gels stabilized by a low-molecular weight organogelator dehydroabietic acid*, Langmuir, 2022.

[32] M. Katarzyna and Z. Dawid, "New derivatives of 4′-phenyl-2,2′:6′,2″-terpyridine as promising anticancer agents," *European Journal of Medicinal Chemistry*, vol. 212, p. 113032, 2021.